JOURNAL OF MATERIALS SCIENCE 31 (1996) 537–544

The reaction sequence in the synthesis of aluminium borate whiskers

H. WADA, K. SAKANE, T. KITAMURA
Shikoku National Industrial Research Institute, 2217-14 Hayashi-cho, Takamatsu-shi, Kagawa 761-03, Japan*

H. HATA
Shikoku Chemicals Corporation, Minato-machi, Marugame-shi, Kagawa 763, Japan

The reaction sequences in the synthesis of aluminium borate whiskers from the raw material mixtures ($Al_2(SO_4)_3/H_3BO_3/K_2SO_4$, K_2SO_4 as a flux) were investigated by differential thermal analysis–thermogravimetric analysis (DTA–TG), X-ray diffraction analysis (XRD), and a direct observation of the reacting mixture. DTA of a mixture with the optimum composition for obtaining well-grown whiskers with a high yield, and XRD of the same mixtures quenched at various temperatures, showed that the reaction proceeds through formation and decomposition of double salts of aluminium: first tripotassium aluminium sulphate and then monopotassium aluminium sulphate. This reaction sequence and the DTA results of mixtures with different $K_2SO_4/(Al+B)$ ratios were successfully explained by the phase diagram of the $Al_2(SO_4)_3$–K_2SO_4 system. Direct observation of the reacting mixture confirmed the explanation. The compositions of reacting mixtures were then calculated from the TG data and traced on the phase diagram. The tracing showed that the decomposition of aluminium salts occurred in different physical states, depending on the $K_2SO_4/(Al+B)$ ratio, in solid, solid and then liquid, or liquid phase. This difference in decomposition explained well the effect of the $K_2SO_4/(Al+B)$ ratio on the morphology of the whiskers. The effect of the B/Al ratio in the mixture was similarly explained by the correlated change in the K_2SO_4/Al ratio.

1. Introduction

Aluminium borate ($9Al_2O_3 \cdot 2B_2O_3$, abbreviated as 9A2B) is a refractory compound with a melting point of 1713 K [1] and a low density of 2.94 g cm^{-3}. It has a crystal structure similar to that of andalusite [2], and physical and optical properties analogous to mullite [1], the structure of which is also similar to andalusite. Because of this crystal structure, 9A2B tends to form needle-shaped crystals. By utilizing this tendency, the whiskers of this compound have been synthesized from aluminium sulphate and boric acid in potassium sulphate flux [3]. The conditions for the synthesis were also investigated, including the B/Al and $K_2SO_4/(Al + B)$ ratios in the raw material mixture, the heating temperature, and the heating time [4]. On the basis of this investigation, a B/Al ratio of 2/8, a $K_2SO_4/(Al + B)$ ratio of 1, and a heating temperature of 1373 K were found to be optimum in respect of the phase purity of the product, the morphology of whiskers, and the yield. Without the K_2SO_4 flux, only a powdery product with a submicrometre size could be obtained, whereas by increasing the amount of flux, the size of the whiskers remarkably increased. The size of the whiskers also increased with an increasing B/Al ratio. On the other hand, the heating time at 1373 K had no effect on the morphology or yield. This last result shows that the reaction sequence in heating the raw material mixture up to the heating temperature determines the morphology of the whiskers and the yield; soaking in molten K_2SO_4 does not grow 9A2B whiskers. This result is different from that obtained with magnesium pyroborate whiskers, which grow in molten KCl through the dissolution–precipitation mechanism [5]. Therefore, in order to control whisker morphology, the reaction sequence in heating the raw material mixture and its relation to the crystal growth of 9A2B should be clarified. In the present work, the reaction sequence was investigated by differential thermal and thermogravimetric analysis (DTA–TG), X-ray diffraction analysis (XRD), and a direct observation of a reacting mixture, with a phase diagram of the $Al_2(SO_4)_3$–K_2SO_4 system.

*Previously known as the Government Industrial Research Institute, Shikoku.

0022–2461

2. Experimental procedure

Aluminium sulphate (chemical grade) and potassium sulphate (guaranteed reagent) were pulverized in a pot mill for 1 day, and with boric acid (guaranteed reagent) in a vibrating mill for 5 h. The aluminium sulphate was then dried at 403 K for 4 h. These reagents were mixed in B/Al ratios ranging from 1/9 to 6/4, and $K_2SO_4/(Al + B)$ ratios ranging from 0 to 2.5. The mixture was further pulverized in the pot mill for 1 h and sieved with a screen having an aperture size of 0.4 mm for homogenizing.

DTA–TG of these mixtures were conducted with an apparatus for thermal analysis (Thermoflex, Rigaku), to which a homemade data-handling system was added. The outputs of DTA, TG, and the temperature were led to a data logger, where they were digitized. These digitized data were then transferred from the logger to a personal computer for further data processing. The conditions for the analyses were as follows: sample weight, about 35 mg; sample pan, platinum; reference material, alumina powder; heating rate, 10 K min^{-1}; atmosphere, air. The DTA signal was normalized with the sample weight, while the TG signal was normalized with the theoretical weight loss, which was calculated on the following assumptions: the total reaction is expressed by Equation 1 and the weight loss is due to the dissipations of SO_3 and H_2O only.

$$x\,Al_2(SO_4)_3 + y\,H_3BO_3 + z\,K_2SO_4 \rightarrow x\,Al_2O_3 + (y/2)\,B_2O_3 + z\,K_2SO_4 + (3x)\,SO_3 + (3y/2)\,H_2O \quad (1)$$

In the following sections, the temperature for each thermal reaction is expressed by its peak temperature.

Some of the mixtures were also heated to predetermined temperatures and quenched with liquid nitrogen. The heating was conducted with the DTA furnace to confirm the completion of each thermal reaction. The quenched samples were then identified by X-ray diffraction analysis with a diffractometer (RAD IIa, Rigaku) using CuK_α radiation. The diffraction data were smoothed with the Savitzky– Golay algorithm [6] before plotting.

The phase change of the mixture during heating was also observed with a furnace and a video camera system. The furnace (KDF VAN 7, Denken, partly modified) had an observation hole in the front panel, in which a quartz disc was inserted as a window to prevent heat loss by convection. Another hole was located in the top wall, through which a Pt–PtRh(13%) thermocouple was inserted to measure the temperature near the sample (hereafter referred to as the sample temperature). The sample was put in a small test tube of quartz with an inner diameter of 4 mm and a length of 10 mm. This tube was supported with a Pt–PtRh(13%) wire with a diameter of 0.5 mm and placed at the centre of the furnace. The sample was illuminated through the front hole with a fibre light source with a halogen lamp and observed with a CCD camera fitted with a telephoto lens. The video output of the camera was then input to a video tape recorder and displayed on a monitor. The temperature control system of the original furnace was replaced with a programmable controller (SU12, Chino) for precise temperature control. The sample temperature was digitized with a data logger and recorded in an interval of 5 s. The heating rate of the furnace was set at 10 K min^{-1} and the sample was heated in air to 1373 K.

3. Results and discussion

3.1. Reaction sequence in heating

The DTA–TG curve of the mixture with B/Al = 2/8 and $K_2SO_4/(Al + B) = 1$ is shown in Fig. 1. The mixture with this composition gave well-grown $9Al_2O_3{\cdot}2B_2O_3$ whiskers with a high yield [4]. Fig. 1 shows seven endothermic peaks and one exothermic peak; 395 K, 602 K, 859 K, 879 K, 950 K, 1184 K, 1383 K (endo), and 805 K (exo). The endothermic peaks at 395 K and 1184 K were accompanied by weight loss. The former peak was identified as the unresolved two dehydrations of boric acid, from literature data (lit.) [7] and the DTA–TG result (obs.) with boric acid. However the latter reaction could not be identified in the same way from the DTA–TG results with each component in the mixture. The decomposition of aluminium sulphate (obs. 1136 K) was the closest in temperature to the reaction, but the temperature difference between them was still too large to identify. In addition, this peak was composed of several sharp and badly reproducible peaks (though for clarity these peaks are not shown in Fig. 1), showing a clear contrast with one broad peak in the decomposition of aluminium sulphate. The two endothermic peaks without weight loss at 859 K and 1383 K were identified as the phase transition from orthorhombic to hexagonal potassium sulphate (lit. 856 K [8]; obs. 846 K) and the melting of potassium sulphate (lit. 1342 K [8]; obs. 1387 K), respectively. The endothermic peak at 950 K has already been identified as the melting of an intermediate product of tripotassium aluminium sulphate, $K_3Al(SO_4)_3$ [3, 9]. The other

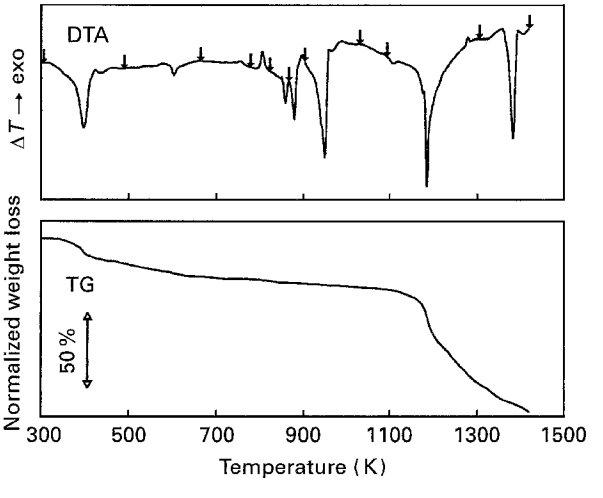

Figure 1 DTA and TG curves of $Al_2(SO_4)_3/H_3BO_3/K_2SO_4$ mixture with optimum composition for $9Al_2O_3 \cdot 2B_2O_3$ whisker synthesis; B/Al = 2/8 and $K_2SO_4/(Al + B) = 1$. For arrows, see text.

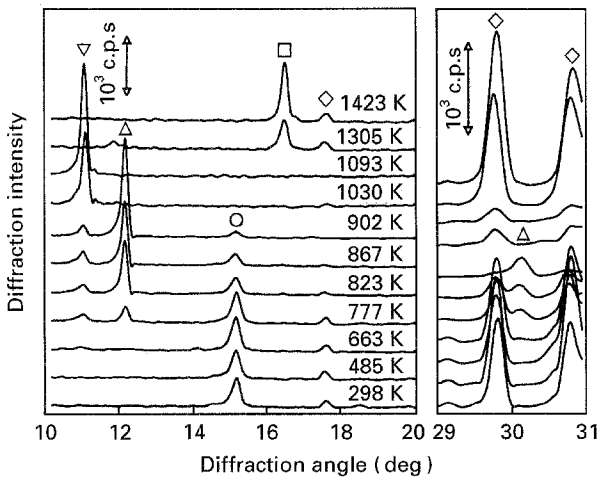

Figure 2 X-ray diffraction patterns of the mixtures with optimum composition heated to the temperatures indicated by arrows in Fig. 1. The marks indicate diffraction lines of (○) $Al_2(SO_4)_3$, (◇) K_2SO_4, (▽) $KAl(SO_4)_2$, (△) $K_3Al(SO_4)_3$, and (□) 9A2B.

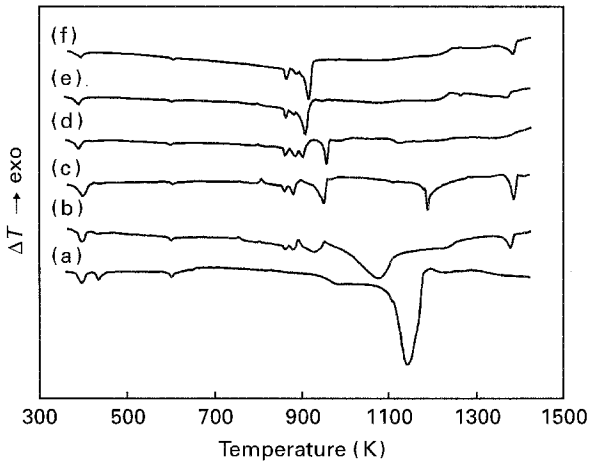

Figure 3 Change of DTA curve of $Al_2(SO_4)_3/H_3BO_3/K_2SO_4$ mixture with $K_2SO_4/(Al + B)$ ratio under a fixed B/Al ratio of 2/8. $K_2SO_4/(Al + B)$: (a) 0, (b) 0.5, (c) 1, (d) 1.5, (e) 2, (f) 2.5.

peaks at 602 K, 879 K and 805 K could not be identified from the above DTA–TG data. The TG curve shows a gradual weight loss between 420 K and 870 K. This is probably due to slow dissipation of residual water in dehydrated boric acid, for the dehydrated product of boric acid is usually glassy B_2O_3 and it easily interferes with further dehydration. However, another possibility that should not be excluded is that the adsorbed water on aluminium sulphate was gradually removed by heating.

The sequence of reactions in heating the same mixture was further examined by X-ray diffraction analysis of the heated mixtures. Fig. 2 shows the diffraction patterns of the mixtures which were heated to the temperatures marked with arrows in Fig. 1 and then quenched with liquid nitrogen. There were five compounds identified by XRD: aluminium sulphate, potassium sulphate, tripotassium aluminium sulphate (hereafter referred to as tripotassium salt), monopotassium aluminium sulphate ($KAl(SO_4)_2$, referred to as monopotassium salt), and aluminium borate. Boric acid was not detected in the samples even before heating, owing to its relatively low concentration and the weak scattering powers of its constitutive elements. From room temperature to 663 K, only diffraction peaks of the raw materials, $Al_2(SO_4)_3$ and K_2SO_4, were observed. At 777 K, two new compounds appeared: monopotassium salt and tripotassium salt. These are the double salts of aluminium sulphate and potassium sulphate in the mole ratios of 1/1 and 1/3, respectively. Then with increasing temperature, the diffraction intensity of tripotassium salt increased, while those of aluminium sulphate and potassium sulphate decreased. At 902 K, the diffraction peaks of aluminium sulphate almost disappeared and those of potassium sulphate disappeared completely. These results show that tripotassium salt was formed from aluminium sulphate and potassium sulphate between 777 and 902 K. At 1030 K, the diffraction peaks of the tripotassium salt disappeared and that of the monopotassium salt increased abruptly. These changes agree well with the melting of tripotassium salt at 950 K shown in Fig. 1 and clearly show that the melting was incongruent to form monopotassium salt. At 1305 K, the diffraction peaks of monopotassium salt also disappeared and that of aluminium borate appeared with potassium sulphate.

The results in Figs 1 and 2 are summarized in the following reaction sequence (Equations 2–6).

$$2H_3BO_3 \rightarrow B_2O_3 + 3H_2O \quad (395\text{–ca.}870\ K) \quad (2)$$

$$Al_2(SO_4)_3 + 3K_2SO_4 \rightarrow 2K_3Al(SO_4)_3 \quad (777\text{–}902\ K) \quad (3)$$

$$K_3Al(SO_4)_3 \rightarrow KAl(SO_4)_2 + K_2SO_4 \quad (950\ K) \quad (4)$$

$$2KAl(SO_4)_2 \rightarrow Al_2O_3 + K_2SO_4 + SO_3 \quad (1184\text{–}1423\ K) \quad (5)$$

$$9Al_2O_3 + 2B_2O_3 \rightarrow 9Al_2O_3 \cdot 2B_2O_3 \quad (1184\text{–}1423\ K) \quad (6)$$

The overall reaction is also given by Equation 7.

$$9Al_2(SO_4)_3 + 4H_3BO_3 \rightarrow 9Al_2O_3 \cdot 2B_2O_3 + 6H_2O + 27SO_3 \quad (7)$$

These equations show that potassium sulphate flux is not a simple reaction medium but a kind of catalyst participating in the reactions. This is, without doubt, one reason why potassium sulphate is a superior flux to potassium chloride for synthesizing 9A2B whiskers [3].

3.2. Effect of amount of flux on reaction sequence

DTA curves of the mixtures with different amounts of the flux ($K_2SO_4/(Al + B)$ ratios) and with a fixed B/Al ratio of 2/8 are shown in Fig. 3. The DTA curves of the mixtures were markedly changed by the $K_2SO_4/(Al + B)$ ratio. The mixture with $K_2SO_4/(Al + B) = 0$ showed a simple DTA curve (Fig. 3a). In addition to two dehydration peaks of boric acid at 393 K and 432 K, two endothermic peaks at 600 K and 1140 K were seen. The former was ascribed to an impurity in aluminium sulphate, because it was observed also for

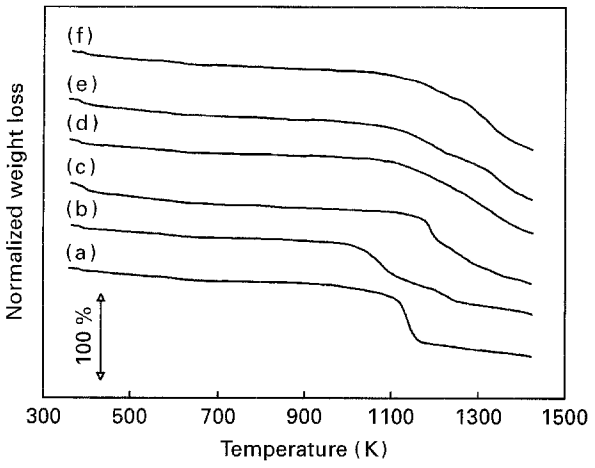

Figure 4 Change of TG curve of $Al_2(SO_4)_3/H_3BO_3/K_2SO_4$ mixture with $K_2SO_4/(Al + B)$ ratio under a fixed B/Al ratio of 2/8. $K_2SO_4/(Al + B)$: (a) 0, (b) 0.5, (c) 1, (d) 1.5, (e) 2, (f) 2.5.

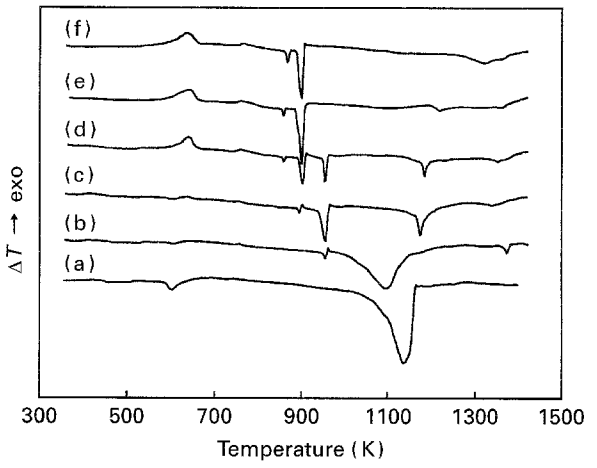

Figure 5 Change of DTA curve of $Al_2(SO_4)_3/K_2SO_4$ mixture with K_2SO_4/Al ratio: (a) 0, (b) 0.5, (c) 1, (d) 1.5, (e) 2, (f) 3.

aluminium sulphate. The latter peak corresponds to thermal decomposition of aluminium sulphate, which was confirmed by DTA–TG of aluminium sulphate. An increase of the $K_2SO_4/(Al + B)$ ratio to 0.5 dissipated the decomposition peak and developed new endothermic peaks: two small peaks at 859 K and 879 K, two broad peaks at about 920 K and 1070 K, and a sharp peak at 1377 K (Fig. 3b). As described in the previous section, the first and the last peaks are due to the phase transition and the melting of potassium sulphate, respectively. Further increase of the $K_2SO_4/(Al + B)$ ratio to 1 then dissipated the two broad peaks and developed two new peaks at 950 K and 1184 K (Fig. 3c, the same as Fig. 1). These two peaks have already been identified in the previous section as the melting of tripotassium salt and the decomposition of monopotassium salt, respectively. The increase of the $K_2SO_4/(Al + B)$ ratio to 1.5 showed another interesting change in the DTA curve (Fig. 3d). The decomposition peak of monopotassium salts diffused away and a small endothermic peak appeared at 900 K. This peak shifted to a higher temperature and became larger with increasing $K_2SO_4/(Al + B)$ ratio. Another remarkable change was the disappearance of the melting peak of tripotassium salt at 950 K at $K_2SO_4/(Al + B) \geqslant 2$ (Fig. 3e).

TG curves of the same samples are shown in Fig. 4. The mixture with $K_2SO_4/(Al + B) = 0$ showed one clear weight loss at 1140 K due to the decomposition of aluminium sulphate (Fig. 4a). An increase of the $K_2SO_4/(Al + B)$ ratio to 0.5 split the weight loss into two steps, one at lower and the other at higher temperature (Fig. 4b), although the second reaction was not clearly detected in the DTA curve. By further increase of the $K_2SO_4/(Al + B)$ ratio to 1 (Fig. 4c), the two steps were unified again into one weight loss, the temperature of which was in the middle of those of the two steps but higher than that for the mixture with $K_2SO_4/(Al + B) = 0$. The comparison with other TG curves shows this weight loss was very fast in the early stage and then gradually slowed down in the following stage. When the $K_2SO_4/(Al + B)$ ratio increased to more than 1, the beginnings of weight loss shifted to

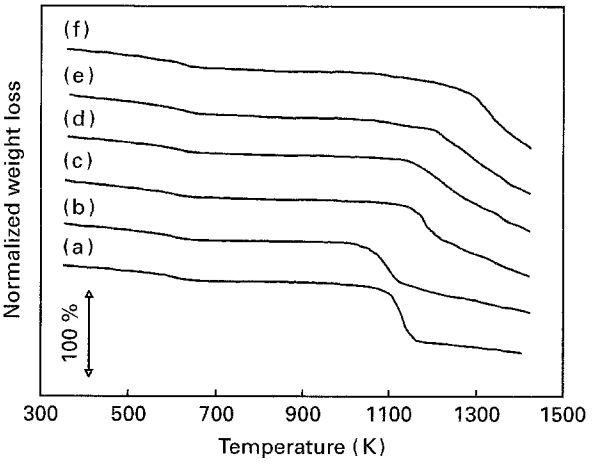

Figure 6 Change of TG curve of $Al_2(SO_4)_3/K_2SO_4$ mixture with K_2SO_4/Al ratio: (a) 0, (b) 0.5, (c) 1, (d) 1.5, (e) 2, (f) 3.

a lower temperature, though it could not be observed clearly (Fig. 4d–f).

There was only a little boric acid in the mixtures under the experimental conditions (B/Al = 2/8 and $K_2SO_4/(Al + B) = 0$–2.5), and hence it probably did not greatly affect the reaction sequence during heating the mixtures. This expectation was examined by comparing the above DTA–TG results with those of the mixtures without H_3BO_3, i.e. $Al_2(SO_4)_3/K_2SO_4$ mixtures, which are shown in Figs 5 and 6. The comparison between the two DTA results (Figs 3 and 5) showed a general similarity in thermal reactions. In particular, the changes of the DTA curves from 800 K to 1300 K with the $K_2SO_4/(Al + B)$ or K_2SO_4/Al ratio were nearly the same. The major differences between the two results were the dehydration peaks of boric acid at 393 K and 432 K, observed only for the $Al_2(SO_4)_3/H_3BO_3/K_2SO_4$ mixtures, and a broad exothermic peak at about 640 K, only for $Al_2(SO_4)_3/K_2SO_4$ mixtures. The latter peak was identified as due to the formation of tripotassium salt by XRD of the quenched samples. These differences, however, probably did not affect the reaction sequence above 800 K, because tripotassium salt also formed in

the $Al_2(SO_4)_3/H_3BO_3/K_2SO_4$ mixtures, though gradually from 777 to 902 K, and the DTA curves of the two mixtures were nearly the same at temperatures from 800 to 1300 K. The minor differences were the presence of an unidentified small endothermic peak at 879 K and a shift of the endothermic peak at 900 K to a higher temperature with an increasing K_2SO_4/Al ratio, which were observed only for the $Al_2(SO_4)_3/H_3BO_3/K_2SO_4$ mixtures. A comparison of the two series of TG curves (Figs 4 and 6) also showed a close similarity between the corresponding TG curves and consequently in their change with the $K_2SO_4/(Al + B)$ or K_2SO_4/Al ratio. Although there remained slight differences between the two DTA–TG results, the effect of coexisting boric acid on the reaction sequence up to the decomposition of the aluminium salts, was found to be small.

The finding described in the previous paragraph opened up the possibility that the DTA results shown in Fig. 3 could be explained by employing the phase diagram of the $Al_2(SO_4)_3$–K_2SO_4 system. The phase diagram [10] is shown in Fig. 7. Although the original diagram involved some uncertainty due to the limited experimental points, the diagram in Fig. 7 was drawn in a definitive way. The diagram shows that the system has a eutectic point at 15 mol% $Al_2(SO_4)_3$ and 893 K and accordingly a liquid phase at temperatures above 893 K. The diagram also shows that the system involves two double salts from aluminium sulphate and potassium sulphate, i.e. tripotassium aluminium sulphate and monopotassium aluminium sulphate, and that they melt incongruently at 953 K and 1053 K, respectively. The original diagram also showed that the phase transition of tripotassium salt occurs at 633 K. On the phase diagram in Fig. 7, the $Al_2(SO_4)_3/(Al_2(SO_4)_3 + K_2SO_4)$ ratios in the respective mixtures were marked with arrows. The comparison of DTA results in Fig. 3 with the phase diagram showed that the endothermic peak at 900 K was due to the eutectic reaction of potassium sulphate and tripotassium salt. The presence of this peak only in the mixtures with $K_2SO_4/(Al + B) \geqslant 1.5$ is coincident with the expectation of the phase diagram. The shift of this peak to a higher temperature with an increasing $K_2SO_4/(Al + B)$ ratio would have been due to the presence of glassy B_2O_3, because such a shift was not observed for the $Al_2(SO_4)_3/K_2SO_4$ mixtures. The glassy B_2O_3 probably interfered with the contact between K_2SO_4 and $K_3Al(SO_4)_3$ and delayed the completion of the eutectic reaction. The phase diagram also showed clearly that the peak at 950 K was due to the incongruent melting of tripotassium salt. On the other hand, the incongruent melting of monopotassium salt at 1053 K shown in the phase diagram was not found in the DTA results. DTA–TG results (Figs 3b and 4b) and XRD on quenched samples showed that the broad endothermic peak at 1074 K observed in the mixture with $K_2SO_4/(Al + B) = 0.5$ was due to the decomposition of monopotassium salt. In the mixture with $K_2SO_4/(Al + B) = 1$, monopotassium salt remained even in the sample heated to 1093 K (Fig. 2i) and ultimately decomposed at 1184 K. This discrepancy was not due to the presence of the glassy B_2O_3, because the $Al_2(SO_4)_3/K_2SO_4$ mixtures gave the same results (Fig. 5). It may be due to the difference between the property of equilibrium in the phase diagram and the kinetic nature in the DTA data. In spite of this discrepancy, the DTA results of the $Al_2(SO_4)_3/H_3BO_3/K_2SO_4$ mixtures are well explained by the phase diagram of the $Al_2(SO_4)_3$–K_2SO_4 system.

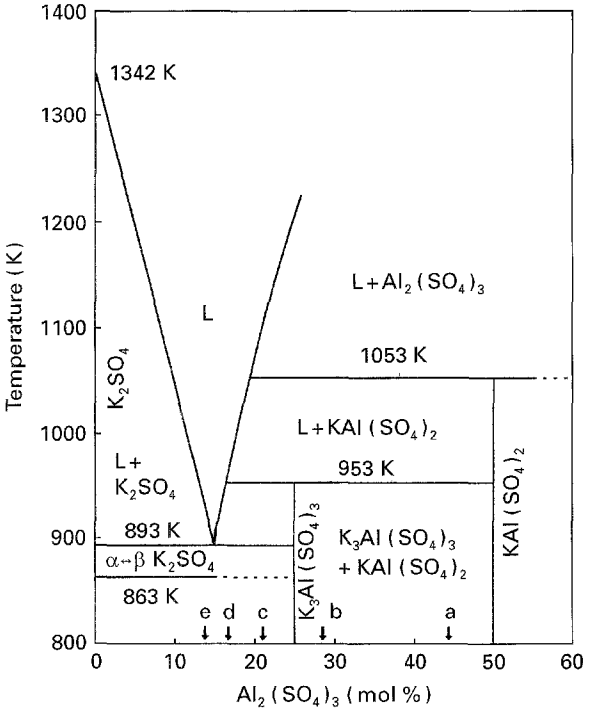

Figure 7 Phase diagram of $Al_2(SO_4)_3$–K_2SO_4 system [10]. Arrows indicate the compositions corresponding to $Al_2(SO_4)_3/H_3BO_3/K_2SO_4$ mixtures with $K_2SO_4/(Al + B)$ ratios of (a) 0.5, (b) 1, (c) 1.5, (d) 2, (e) 2.5.

3.3. Relation between reaction sequence and morphology of whiskers

The reaction sequences in heating the raw material mixtures can be estimated by the phase diagram of the $Al_2(SO_4)_3$–K_2SO_4 system, on the basis of the discussion in the previous section. We therefore tried to trace each sequence on the phase diagram using the TG data of Fig. 4. The following assumptions were used for the tracing: (1) the mole fraction of H_3BO_3 or B_2O_3 in the reacting mixture is small. Consequently, the physical state of the mixture, i.e. a solid or liquid state, is determined only by the $Al_2(SO_4)_3/(Al_2(SO_4)_3 + K_2SO_4)$ ratio; (2) The dehydration of H_3BO_3 is completed before the sample temperature reaches 870 K and accordingly all the weight loss above 870 K is due to the decomposition of aluminium salts, i.e. aluminium sulphate or monopotassium salt. Then the mole fraction of aluminium sulphate, $Al_2(SO_4)_3/(Al_2(SO_4)_3 + K_2SO_4)$, in a reacting mixture can be calculated at each temperature from the normalized TG curve. These values are plotted on the phase diagram in Fig. 8. The compositional change in the mixture with $K_2SO_4/(Al + B) = 0.5$ occurred in two stages. The first was due to the decomposition of

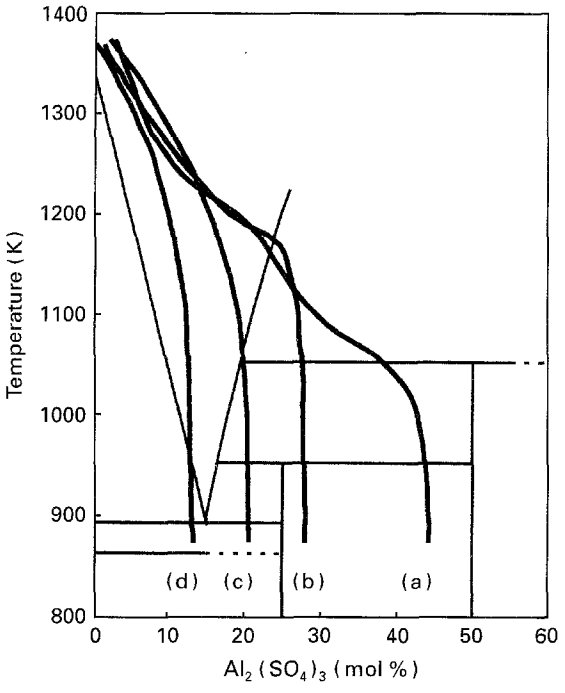

Figure 8 Changes of $Al_2(SO_4)_3/(Al_2(SO_4)_3 + K_2SO_4)$ mole ratios in heating $Al_2(SO_4)_3/H_3BO_3/K_2SO_4$ mixtures with a B/Al ratio of 2/8 and $K_2SO_4/(Al + B)$ ratio of (a) 0.5, (b) 1, (c) 1.5 and (d) 2.5.

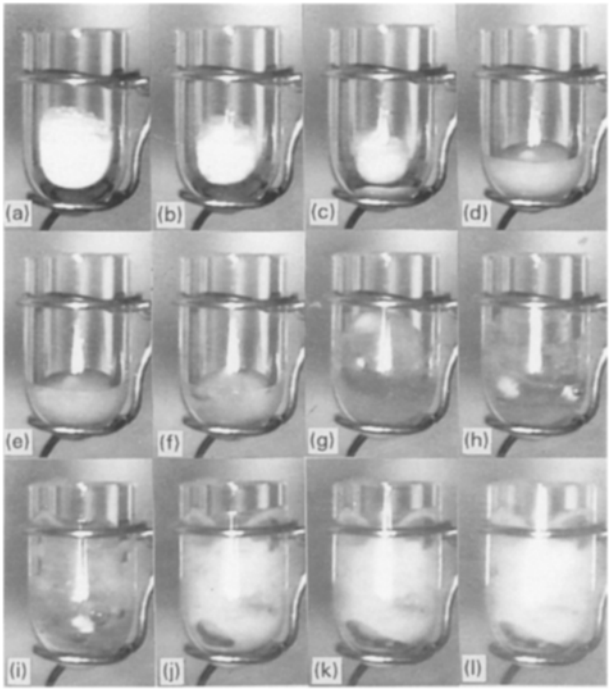

Figure 9 Appearance of $Al_2(SO_4)_3/H_3BO_3/K_2SO_4$ mixture with a B/Al ratio of 2/8 and a $K_2SO_4/(Al + B)$ ratio of 1 at the temperatures of (a) 298 K, (b) 923 K, (c) 943 K, (d) 973 K, (e) 1023 K, (f) 1073 K, (g) 1103 K, (h) 1123 K, (i) 1143 K, (j) 1173 K, (k) 1223 K, and (l) 1273 K.

monopotassium salt in the solid phase and the second was due to that of aluminium sulphate in liquid phase (Fig. 8a). By contrast, the mixture with $K_2SO_4/(Al + B) = 1$ decomposed almost solely in the liquid phase. It is interesting that the decomposition started just at the temperature at which all the mixture became liquid. Further increase in the $K_2SO_4/(Al + B)$ ratio lowered this temperature. Under this situation, the decomposition started at a lower temperature and proceeded slowly in the liquid phase (Fig. 8c and d). These results show that the phase in which the aluminium salts decomposed was different for mixtures with different $K_2SO_4/(Al + B)$ ratios.

The formation of the liquid phase and the decomposition of aluminium sulphate in the liquid phase were confirmed further by direct observation of the reactions. The change in appearance of the mixture with $K_2SO_4/(Al + B) = 1$ is shown in Fig. 9. The appearance of the mixture did not change until the temperature reached 943 K, except in the reduction of its apparent volume. At 973 K, some liquid phase developed but solid phase also remained. With increasing temperature the amount of the liquid phase increased. At 1123 K, the mixture became an almost transparent liquid. At the nearly same temperature, bubbles started to evolve and the bubbling was the most intense at about 1143 K. This bubbling corresponds well with the rapid weight loss in the TG curve and also the badly reproducible peaks in the DTA curve, although the temperature of the observation is about 40 K lower than that in the DTA–TG results (1184 K). This discrepancy may be due to the difference in the position of measuring the sample temperature: the immediate vicinity of the sample tube in the observation. At 1173 K, white materials precipitated and the mixture became non-transparent again. These precipitates were identified as $9Al_2O_32B_2O_3$ by XRD (Fig. 2j). Thus the direct observation of the reacting mixture supports the expectation from the phase diagram.

The differences in phase and temperature for the decomposition of the aluminium salts should affect the morphology of its product, $9Al_2O_3{\cdot}2B_2O_3$ whiskers. The mixture with $K_2SO_4/(Al + B) = 0$ had no liquid phase in the reaction sequence except a small amount of B_2O_3 melt. In this circumstance, it was difficult for crystal nuclei of 9A2B to grow sufficiently; only small crystals were obtained. In the mixture with $K_2SO_4/(Al + B) = 0.5$, the first decomposition occurred in the solid phase and consequently would have created small 9A2B crystals. These crystals could grow in the liquid phase during the second decomposition. However, many crystals had been created by the first decomposition. As a result, the mass of $9Al_2O_3{\cdot}2B_2O_3$ produced by the second decomposition and the following reaction with B_2O_3 was insufficient for all these crystals to grow sufficiently. This situation also gave small whiskers. On the other hand, in the mixtures with $K_2SO_4/(Al + B) = 1.5$–2.5, the decomposition proceeded slowly in liquid phase from a relatively low temperature. In this case a small number of nuclei would have formed at a low temperature and they grew gradually in liquid phase, resulting in large whiskers with widely distributed sizes. In the middle composition between them, i.e. at $K_2SO_4/(Al + B) = 1$, the very early stage of decomposition possibly occurred in the solid phase but it was immediately followed by fast decomposition in the liquid phase. The fast decomposition probably created many crystal nuclei of 9A2B as in the mixture with

$K_2SO_4/(Al + B) = 0.5$. However, the mass of 9A2B produced by the following decomposition was much more than that in the other case, allowing those nuclei to grow sufficiently. The bubbling caused by the fast decomposition mixed the liquid phase and stimulated material transport. These circumstances gave well-grown whiskers with a relatively uniform size.

3.4. Effect of B/Al ratio on the reaction sequence and whisker morphology

The morphology of the whiskers was also affected by the B/Al ratio in the respective raw material mixtures; the larger the B/Al ratio used, the larger were the whiskers obtained [4]. This effect could be ascribed simply to the flux action of excess B_2O_3. However, a different experiment on the preparation of $9Al_2O_3{\cdot}2B_2O_3$ from $Al_2(SO_4)_3/H_3BO_3$ mixtures showed that the effect of the B/Al ratio on the morphology of the product was much smaller than that in the preparation from $Al_2(SO_4)_3/H_3BO_3/K_2SO_4$ mixtures. Consequently, another explanation was necessary. One possible explanation was that the change in the morphology was due to the increase in the K_2SO_4/Al ratio with an increasing B/Al ratio under $K_2SO_4/(Al + B) = 1$. This possibility was then investigated with DTA–TG in the same way as the effect of flux amount. The DTA and TG curves of the $Al_2(SO_4)_3/H_3BO_3/K_2SO_4$ mixtures with $K_2SO_4/(Al + B) = 1$ and B/Al = 1/9–6/4, which correspond to $Al_2(SO_4)_3/(Al_2(SO_4)_3 + K_2SO_4) = 0.31$–$0.17$, are shown in Figs 10 and 11, respectively. The compositional changes in the reacting mixtures are also plotted on the phase diagram in Fig. 12. Generally, the change of the DTA curve with the B/Al ratio (Fig. 10) was similar to the change with the $K_2SO_4/(Al + B)$ ratio for $K_2SO_4/(Al + B) \geqslant 1$ (Fig. 3c–f). The peak for the eutectic reaction between K_2SO_4 and $K_3Al(SO_4)_3$ was observed also in Fig. 10 at 889 K for the mixtures with B/Al = 4/6–6/4. The $Al_2(SO_4)_3/(Al_2(SO_4)_3 + K_2SO_4)$ ratios in these mixtures were 0.23–0.17 and were located in the range where the eutectic reaction occurs (Fig. 12a and b). A small unidentified endothermic peak was found at 879 K, but only for the mixtures of B/Al = 1/9–3/7. The peritectic peak of tripotassium salt (lit. 953 K) was also observed for the mixtures with B/Al = 1/9–4/6. This finding agreed with the fact that their $Al_2(SO_4)_3/(Al_2(SO_4)_3 + K_2SO_4)$ ratios were in the range where the peritectic reaction occurs (Fig. 12a–c). However, the peak for the peritectic reaction of monopotassium salt was not found for all these mixtures, as observed for the mixtures with varying amounts of flux. Instead, the endothermic peak for the decomposition of monopotassium salt was again observed at 1184 K for the mixtures with B/Al = 1/9–2/8 and at 1101 K for the mixture with B/Al = 3/7. Except for this discrepancy, the change in the DTA curve with the B/Al ratio was well explained by the phase diagram, even though the amount of B_2O_3 seemed too much to neglect. The change in the TG curve with the increasing B/Al ratio (Fig. 11) was also similar to the change with the increasing $K_2SO_4/(Al + B)$ ratio for $K_2SO_4/(Al + B) \geqslant 1$

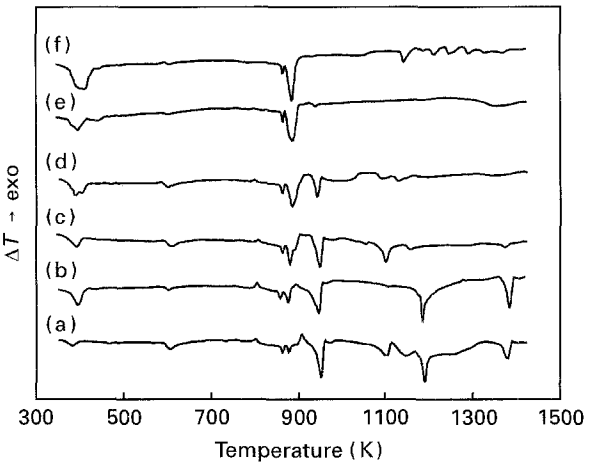

Figure 10 Change of DTA curve of $Al_2(SO_4)_3/H_3BO_3/K_2SO_4$ mixture with B/Al ratio under a fixed $K_2SO_4/(Al + B)$ ratio of 1. B/Al: (a) 1/9, (b) 2/8, (c) 3/7, (d) 4/6, (e) 5/5, (f) 6/4.

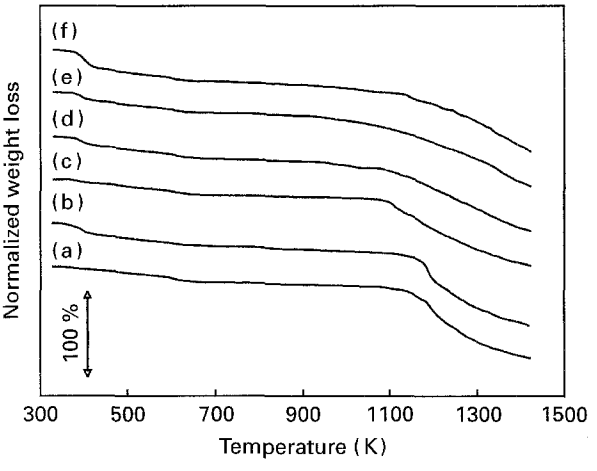

Figure 11 Change of TG curve of $Al_2(SO_4)_3/H_3BO_3/K_2SO_4$ mixture with B/Al ratio under a fixed $K_2SO_4/(Al + B)$ ratio of 1. B/Al: (a) 1/9, (b) 2/8, (c) 3/7, (d) 4/6, (e) 5/5, (f) 6/4.

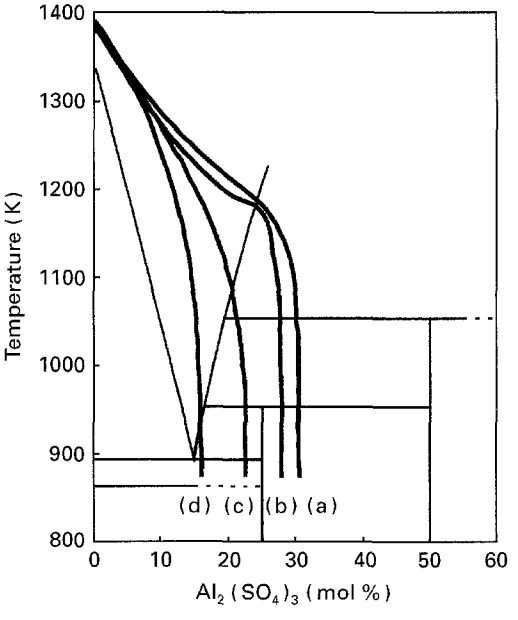

Figure 12 Changes of $Al_2(SO_4)_3/(Al_2(SO_4)_3 + K_2SO_4)$ mole ratios in heating $Al_2(SO_4)_3/H_3BO_3/K_2SO_4$ mixtures with a $K_2SO_4/(Al + B)$ ratio of 1 and B/Al ratio of (a) 1/9, (b) 2/8, (c) 4/6, and (d) 6/4.

(Fig. 4c–f). The temperature at which the weight loss started decreased with the increase of the B/Al ratio from 2/8 to 3/7, and at B/Al $\geqslant$ 4/6 no distinct starting point of decomposition was observed. The tracing of the compositional change on the phase diagram (Fig. 12) showed again that the reacting mixtures with larger B/Al ratios became liquid at a lower temperature and such mixtures started to decompose at a lower temperature.

The change in morphology of $9Al_2O_3{\cdot}2B_2O_3$ whiskers with the B/Al ratio now can be explained by the difference in reaction sequence, similarly to the change in the morphology with flux amount discussed in the previous section. In the mixture with B/Al = 1/9, the reaction proceeded through a course on the phase diagram similar to the mixture with B/Al = 2/8 (Fig. 12a and b), except for the initial rapid decomposition. However, the boron content was only half of the stoichiometric amount for $9Al_2O_3{\cdot}2B_2O_3$, resulting inevitably in α-alumina formation. Thus 9A2B crystal nuclei, formed in the initial stage of decomposition, could not grow sufficiently in the following liquid-phase decomposition. In this situation, only small whiskers were obtained. On the other hand, in mixtures with B/Al = 4/6–6/4, the decomposition started at a lower temperature but proceeded slowly. In this circumstance the crystal nuclei created at lower temperature could grow sufficiently in the following liquid-phase decomposition. This resulted in larger whiskers, as in the mixtures with higher K_2SO_4/(Al + B) ratios. It is interesting to note that the same mechanism can explain both the effects of the flux amount and that of the B/Al ratio.

4. Conclusion

The reaction sequences in heating $Al_2(SO_4)_3/H_3BO_3/K_2SO_4$ mixtures were investigated by DTA–TG, X-ray diffraction analysis, and direct observation of reacting mixtures. From the results, the effects of the K_2SO_4/(Al + B) and B/Al ratios on the morphology of the reaction products, $9Al_2O_3{\cdot}2B_2O_3$ whiskers, were discussed. At the optimum ratios of K_2SO_4/(Al + B) = 1 and B/Al = 2/8, the reaction proceeded through formation and decomposition of double salts of aluminium: first tripotassium aluminium sulphate and then monopotassium aluminium sulphate. DTA results for the mixtures with a varying K_2SO_4/(Al + B) ratio were successfully explained by the phase diagram of the $Al_2(SO_4)_3$–K_2SO_4 system. Tracing the composition of the reacting mixtures on the diagram showed that there were three types of decomposition of aluminium salts: decompositions in solid phase, solid and then liquid phase, and liquid phase. These types of decomposition determined the number of crystal nuclei, the possibility of their growth, and hence the morphology of the whiskers. The effect of the B/Al ratio on the morphology was explained similarly by the correlated change of the K_2SO_4/Al ratio.

References

1. H. SCHOLZE, *Z. Anorg. Allg. Chem.* **284** (1956) 272.
2. M. IHARA, K. IMAI, J. FUKUNAGA and N. YOSHIDA, *Yogyo-Kyokai-Shi* **88** (1980) 77.
3. H. WADA, T. KITAMURA, K. SAKANE, H. HATA and H. KAMBARA, *J. Mater. Sci. Lett.* **10** (1991) 1076.
4. H. WADA, K. SAKANE, T. KITAMURA and H. HATA, *Ceram. Trans.* **25** (1991) 95.
5. K. SAKANE, T. KITAMURA and J. OGAWA, *Gypsum Lime (Jpn)* (216) (1988) 281.
6. A. SAVITZKY and M. J. E. GOLAY, *Anal. Chem.* **36** (1964) 1627.
7. R. W. SPRAGUE, in "Mellor's Comprehensive Treatise on Inorganic and Theoretical Chemistry", Vol. 5, Supp. 1, Part A, ed by R. Thompson and A. J. E. Welch (Longman, London 1980) p. 226.
8. W. P. DOYLE, *ibid.*, Vol. 2, Supp. 3, Part 2 (Longmans, London, 1963) p. 1854.
9. M. M. KAZAKOV, F. L. GLEKEL and N. A. PARPIEV, *Russ. J. Inorg. Chem.* **18** (1973) 788.
10. L. A. KOCHUBEI, E. V. MARGULIS, M. M. SHOKAREV and N. V. PORTVELOVA, *ibid.* **23** (1978) 1255.

Received 2 March 1994
and accepted 22 June 1995